Civil Engineering Infrastructures Journal, 50(1): 151 – 163, June 2017
Print ISSN: 2322-2093; Online ISSN: 2423-6691
DOI: 10.7508/ceij.2017.01.009

Impact of Tamper Shape on the Efficiency and Vibrations Induced During Dynamic Compaction of Dry Sands by 3D Finite Element Modeling

Mehdipour, S.[1] and Hamidi, A.[2*]

[1] M.Sc. Student, School of Engineering, Kharazmi University, Tehran, Iran.
[2] Professor, School of Engineering, Kharazmi University, Tehran, Iran.

Received: 29 Sep. 2016; Revised: 23 Dec. 2016; Accepted: 25 Dec. 2016

ABSTRACT: Dynamic compaction is a soil improvement method which has been widely used for the increase of bearing capacity through stress wave propagation during heavy tamping. The cost and time of project implementation can be effectively curtailed by developing a model that can be used in the design of dynamic compaction operations. The numerical models offered so far are mostly one or two-dimensional, incapable of examining the total effect of wave emission in the soil. This paper involved the three-dimensional finite element program ABAQUS employing Mohr-Coulomb failure criterion for the analysis of dynamic compaction operation. Modeling of impact on soil surface involved an initial velocity applied to the tamper nodes. Flat section and conical shape tampers with various cone angles were modeled and their effects on the efficiency of dynamic compaction for soils with different initial relative densities were investigated. Moreover, variations of peak particle velocity (PPV) induced by flat or conical tamper at different radial distances and soil densities were evaluated. The analyses were done individually for each mode over five consecutive blow counts. Comparison of the results of PPV, crater depth and crater volume for different tampers revealed the effect of tamper shape on efficiency and vibrations induced during dynamic compaction. Increasing the cone angle of conical tampers increased improvement depth and velocity of particles in all radial directions.

Keywords: 3D Finite Element Modeling, ABAQUS, Dry Sandy Soil, Flat And Conical Tamper, Relative Density.

INTRODUCTION

Dynamic compaction is among improvement methods which have been implemented for loose granular soils in recent years. The method was at first employed in 1957 by the Research Laboratory of the UK to evaluate the impact of falling height in degree of compaction of clayey sands (Smoltczyk, 1983). By 1975, Menard introduced it as a desirable method for soil improvement and reported its application in subgrade improving of Nice airport, France. According to Merrifield and Davis (2000), although dynamic compaction has been adopted as a method of improvement for many years, it has been established recently in practical science literature.

In this method, compaction involves heavy weights of 5 to 30 tons thrown freely from

* Corresponding author E-mail: hamidi@khu.ac.ir

height of 5 to 30 meters (Mayne et al., 1984). Since the soil improvement depends on the vibration of its particles, dispersion and damping of stress waves determines the compacted soil area (Bement and Selby, 1997; Ardeshir Behrestaghi et al., 2013; Shafiei and Khaji, 2015; Raoofian Naeeni and Eskandari Ghadi, 2016). A number of researchers, including Lukas (1986) and Luongo (1992) divided the effective factors on efficiency and improvement depth of dynamic compaction into two general categories:

a. The ground-related factors include the type and layering of soil, existence of a hard layer under or on compacted soil, degree of saturation and groundwater level.

b. The equipment-related factors like tamper weight, falling height, tamper base area, tamper shape and number of blows.

Tamper shape is generally cylindrical and flat in most dynamic compaction projects. According to van Impe (1989), tamper shape plays an important role in dynamic compaction process. Feng et al. (2000) proposed new ideas for the tamper shape. They used flat base and conical shape tampers and showed better compaction results using the latter. Laboratory researches were continued by Arslan et al. (2007) to compare the improvement depths of flat and conical tampers. The study revealed more effectiveness of conical tampers against flat ones. The tampers were launched from a fixed height on sandy soil, while calculating the crater width and depth after each fall for sandy soils with three different relative densities. The results indicated that maximum crater depth and area were reached at the end of 10^{th} impact for flat tamper and 4^{th} to 7^{th} impacts for conical one. In fact, average improvement energy for conical tamper was less than half the energy spent to improve the soil by flat tamper. Moreover, the conical tamper yielded a deeper improved layer compared to the flat one.

Another important parameter in dynamic compaction process is peak particle velocity (PPV), which is usually applied to define the threshold criterion of noise and harassment for buildings and public facilities especially in urban areas (Rezaei et al., 2016). The expected magnitude of PPV arising from dynamic compaction should be estimated before conducting operations in situations where there is possibility of damage to adjacent structures or inconvenience of residents (Qiao and Li, 2011; Li et al., 2011). The rate of PPV damping is dependent to the horizontal distance divided by the square root of time. It should also be noted that PPV increases with increase in blow counts due to increase in relative density and stiffness of compacted soil (Ghanbari and Hamidi, 2014; Pourjenabi and Hamidi, 2015).

In this paper, the finite element software ABAQUS was used for three dimensional modeling of dynamic compaction considering different tamper shapes. Variations of crater depth and crater volume were compared for different tamper shapes to investigate vertical and radial efficiencies of dynamic compaction process using flat and conical tampers. Moreover, PPV changes were also considered as another important parameter in designing tamping operations. It should be noted that three dimensional modeling allowed better simulation of tamper geometry and achievement of better results compared to the previous studies using two dimensional or axis-symmetric modeling.

MODELING METHOD

Direct integration using the dynamic Eulerian method was used in present study. In the Eulerian method, as an explicit scheme, new solution at each time step is obtained based on the results of the previous time increment. Different steps of numerical modeling are illustrated in the following sessions.

Simulation of Tamper Impact

The velocity (V) of a freely falling weight from height of H on the ground surface is obtained through the following equation:

$$V = \sqrt{2gH} \quad (1)$$

where g is the gravity acceleration. During modeling, velocity of tamper impact to the ground was imported as an initial condition to the nodes of interface elements and the analysis started. It was essential to define the interface elements for an accurate modeling and energy transfer from the tamper to soil. ABAQUS has the ability to define these elements by applying a frictional coefficient using penalty method. Considering the friction angle (δ) between soil and tamper as $\frac{1}{2}\varphi$ to $\frac{2}{3}\varphi$, the coefficient of friction was determined to be tan(δ), which varied between 0.3 and 0.5. Previous studies by Pourjenabi and Hamidi (2015) and the results of analysis within the above range showed low sensitivity of results to frictional coefficient value at mentioned range. As a result, the coefficient of friction for each type of tamper and any relative density was considered to be $\tan\frac{2}{3}\varphi$.

Damping Parameters

To take into account of damping, the Rayleigh damping model was used as follows:

$$[C] = \alpha[M] + \beta[K] \quad (2)$$

where [C], [M] and [K] are damping, mass and stiffness matrixes, respectively. Moreover, α and β represent the Rayleigh damping constants. If parameter α is zero, the higher modes of vibration will be effective and if β is zero, higher modes leave little effect on damping. As a result, α can be ignored since the higher modes are more effective in dynamic compaction as a dynamic impact problem. Also, the parameter β can be obtained as follows (Ghanbari and Hamidi, 2014):

$$\beta = \frac{2\omega D}{\omega_1 + \omega_n} \quad (3)$$

where D is the damping ratio which was considered as 5%. Also ω_1, ω_n illustrate the frequency range as the minimum and maximum frequencies (0.01 and 100 Hz based on frequency analysis). Moreover, ω is the frequency of vibration which was chosen as 10 Hz in accordance to the results of Pan and Selby (2002) and Hwang and Tu (2006). As a result, the parameter β was determined as 0.01 for the analysis. The time between two successive blows was selected in a way that all energy and particle velocities are damped at the beginning of next blow in the soil body.

Modeling of Soil Behavior

Cap plasticity model has been adopted in several numerical models which have been for dynamic compaction and has showed good consistency and results (Ghassemi et al., 2009; Pourjenabi and Hamidi, 2015). However, determination of required parameters for cap plasticity model requires a number of different experiments which usually is not available for model verification. Pourjenabi et al. (2013) numerically modeled dynamic compaction using different constitutive models and concluded that contrary to the Drucher-Prager model, application of Mohr-Coulomb criterion can successfully predict crater depth values during dynamic compaction. Although, the values are somewhat different with predictions using cap plasticity model, the results proved that it can be successfully applied in numerical modeling, especially in lower blow counts.

Mohr-Coulomb criterion is based on five major input parameters including Young's

modulus (E), Poisson's ratio (v), cohesion (c), friction angle (φ) and dilation angle (ψ) which are all available for Arslan et al. (2007) experiments which have been used in current study for model verification.

To demonstrate this model in three-dimensional plane, a formula based on stress tensor invariants was used as follows:

$$\theta = -\frac{1}{3}\sin^{-1}\left(-3\frac{\sqrt{3}}{2}\frac{J_{3D}}{J_{2D}^{3/2}}\right) \quad (3)$$

$$f = J_1 \sin\varphi + \sqrt{J_{2D}}\cos\theta - \frac{\sqrt{J_{2D}}}{3}\sin\varphi\sin\theta - c\cos\varphi = 0 \quad (4)$$

here, f represents the yield function, θ lies between $-\frac{\pi}{6}$ and $+\frac{\pi}{6}$, J_1 is the first invariant of stress tensor and J_{2D} and J_{3D} are the second and third invariants of deviatoric stress tensor. Angle of dilation (ψ) is another required parameter for modeling which was considered as $\psi = \varphi - 30$ in this study.

Model Verification

Arslan et al. (2007) performed an experimental study to investigate the effect of tamper shape on the efficiency of dynamic compaction process. They prepared models in three relative densities, very loose, loose and medium sand in a box of 1120×760×400 mm. Flat and conical shaped tampers weighted 67 N falling from the height of 2.4 m were used and variation of crater depth with blow counts was recorded. Figure 2 shows schematic shapes of the tampers used in their studies. They used conical tampers with cone angles equal to the friction angle of the considered soil. As a result, tampers with cone angles of 30°, 35° and 40° were applied for very loose, loose and medium sands, respectively. The crater depth values were also compared with results of compacting using flat tampers.

Dynamic compaction tests on three soil densities were numerically modeled by ABAQUS using the soil parameters listed in Table 1. Figure 3 shows variation of crater depth with applied energy during blow counts for three different soil types. In each figure, variations of crater depth with energy are compared between numerical and experimental model of Arslan et al. (2007) for flat and conical tampers. According to the figures, the difference between numerical model and experimental data is allowable and can be mainly attributed to the application of the Mohr-Coulomb failure criterion instead of the cap-plasticity model. Indeed, using cap plasticity model can improve the results if adequate experimental data are available to obtain its parameters.

Table 2 briefly compares the results of numerical modeling with experimental data of Arslan et al. (2007). Based on calculated crater depth values at the 5th blow count, it can be concluded that the numerical model and applied constitutive equation were able to predict crater depth variation during dynamic compaction in a good manner. The highest difference was observed for the flat-bottom tamper used in medium dense sand.

Table 1. Parameters of different soils considered in numerical modeling

Soil Type	φ °	γ (kN/m^3)	ψ°	ν	E (kN/m^2)	c (kN/m^2)
Very loose	29.7	13.0	0	0.25	7500	1.0
Loose	34	13.8	4	0.25	10000	1.0
Medium dense	39	14.7	9	0.25	12000	1.0

Table 2. Comparison of results of numerical modeling and experimental data

Crater Depth at 5th Blow Count (m)	Flat-Bottom Tamper			Conical-Bottom Tamper		
	Very Loose Sand	Loose Sand	Medium Sand	Very Loose Sand	Loose Sand	Medium Sand
Experimental data (Arslan et al., 2007)	0.114	0.075	0.070	0.130	0.103	0.926
Numerical model data	0.110	0.076	0.063	0.130	0.109	0.903
Difference percentage (%)	3.0	1.0	10.0	0.0	5.0	2.0

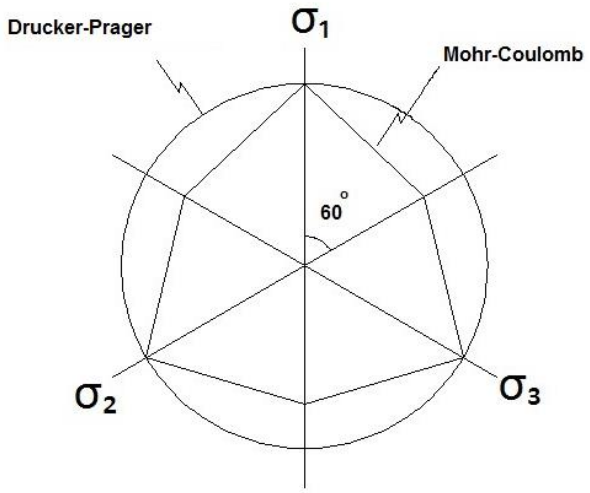

Fig. 1. Mohr-Coulomb criterion on Π plane

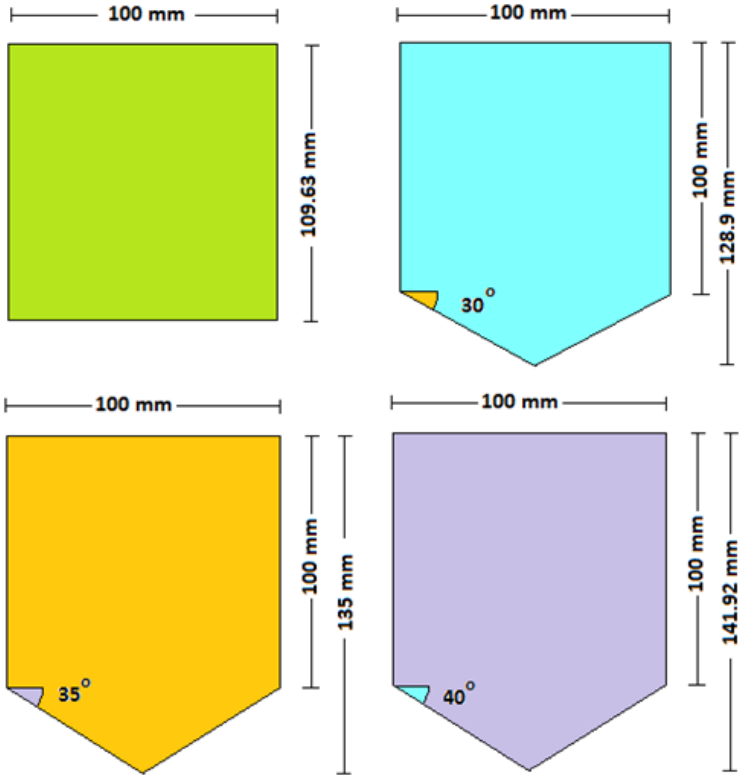

Fig. 2. Schematic shapes of tampers used by Arslan et al. (2007)

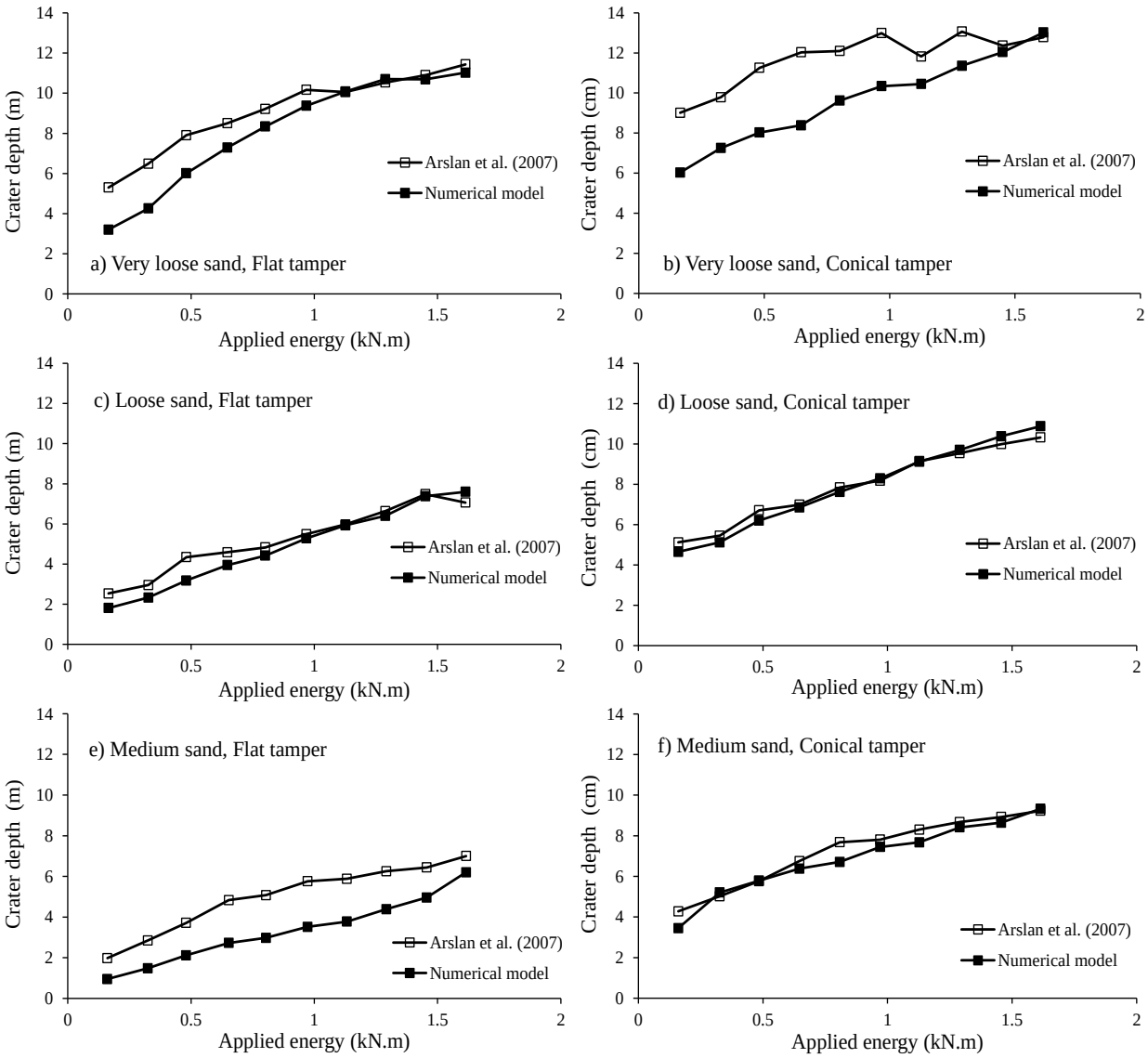

Fig. 3. Verification of numerical model with experimental data of Arslan et al. (2007)

Figure 4 depicts the contours of plastic strain around the tamping point. As the figure clearly shows, the model successfully predicted larger depths of influence for conical tampers compared to the flat one. The strain contours have reached to lower layers of soil when cone angle increased which resulted to better soil improvement. Also it is evident that the depth of influence decreased with increase in relative density. More vertical displacements and strains have occurred in very loose and loose soils compared to that of the medium dense one.

The Main Numerical Model and Analyses

In order to eliminate the effects of boundaries and reflection of the waves back into the model, dimensions of the main model were selected as 40 m thickness, 300 m length and 60 m width. Although, analysis time for the considered large domain was extremely higher than the smaller one used for verification, PPV values at the borders completely vanished, showing elimination of any wave reflection back into the finite element mesh.

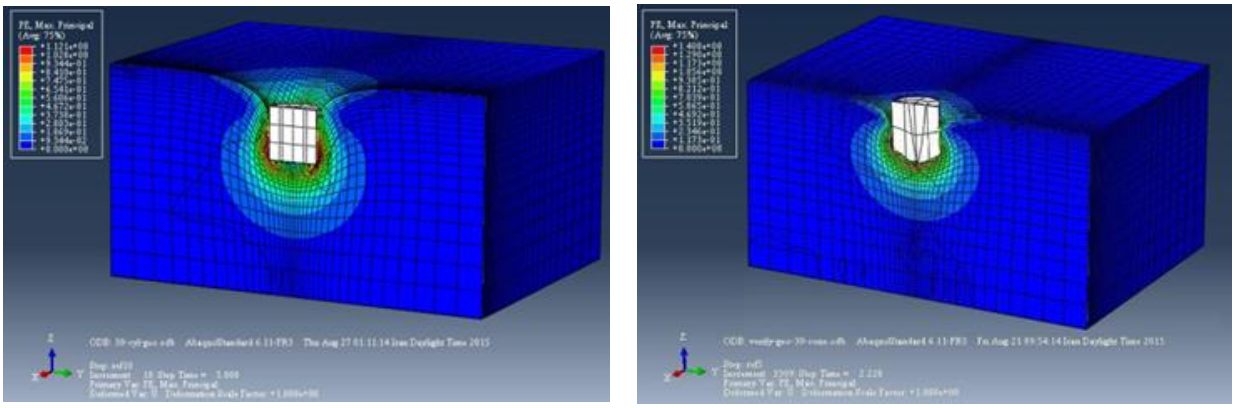

a) Very loose sand, Conical tamper (30°)

b) Very loose sand, Flat tamper

c) Loose sand, Conical tamper (35°)

d) Loose sand, Flat tamper

e) Medium sand, Conical tamper (40°)

f) Medium sand, Flat tamper

Fig. 4. Contours of maximum principal strain for 5th blow count in numerical models of experiments conducted by Arslan et al. (2007)

The soil properties were also selected the same as calibrating phase for three types as listed in Table 1. According to Figure 5, proposed mesh is denser below tamping point and elements size grow by taking distance from tamping centerline. Based on this

hypothesis, elements dimensions ranged from 0.34 to 10 m in numerical model.

Numerical modeling was continued up to five successive blows for each model. One flat and three conical tampers with cone angle (α) identical to the friction angle (φ) and 2˚ less or more ($\varphi \pm 2^{\circ}$) were considered for each soil type. All tampers were selected of identical weight of 30 tons and falling height of 20m from the gravity center to the ground surface. As a result, the same energy was transferred from different tampers to the soil. Elasticity modulus of tampers was considered as 235×10^{8} kPa while Poisson's ratio was set as 0.2. Table 3 displays the specifications of tampers used for each soil type.

Table 3. Specifications of tampers used in the numerical analysis

Soil Type	Tamper Type	α°	H (m)
Very loose sand	Flat	0	1.00
	Conical 28˚	28	1.64
	Conical 30˚	30	1.69
	Conical 32˚	32	1.75
Loose sand	Flat	0	1.00
	Conical 33˚	33	1.78
	Conical 35˚	35	1.84
	Conical 37˚	37	1.90
Medium sand	Flat	0	1.00
	Conical 38˚	38	1.94
	Conical 40˚	40	2.01
	Conical 42˚	42	2.08

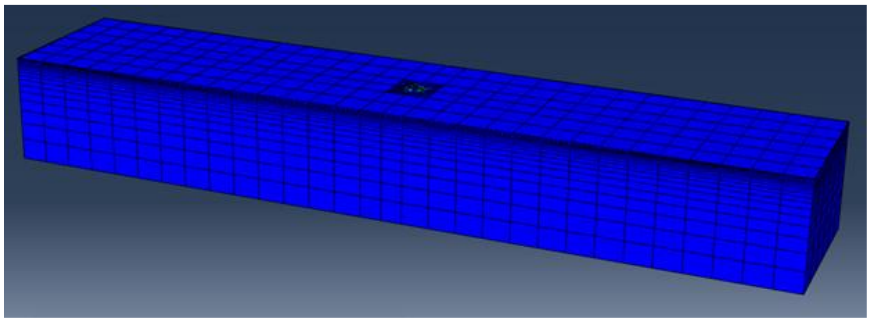

Fig. 5. Numerical model and Finite Element mesh

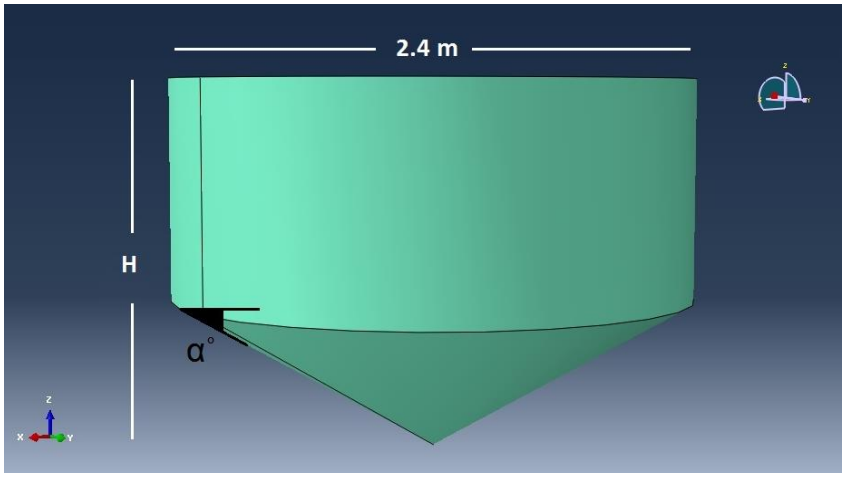

Fig. 6. Conical tamper and its variables used in numerical modeling

RESULTS OF ANALYSES

During dynamic compaction, crater depth of tamper is dependent to the applied energy per unit area. The impact energy, E can be defined by the following equation, where N is the number of blow counts, W is the tamper weight and A is the contact area of soil and tamper:

$$E = \frac{NWH}{A} \quad (6)$$

Figure 7 displays the comparison between crater depths of flat and conical tampers. The results for all three soil types evidently reveal the increase in crater depth by increase in applied energy. As the contact area between soil and tamper decreases, there will be greater penetration in the soil. Averagely for very loose soil, conical tampers experience 42.4% times increase in crater depth compared to flat one at the same tamping energy. This ratio was 58.7% for loose sand and 70.5% for the Medium dense soil.

Figure 8 shows variation of crater volume at 5th blow count versus cone angle for different soil types. It is absolutely clear that the volume of crater decreases by over 30% in all soils with changing the shape of tamper from flat to conical. However, for conical tampers, it decreases more smoothly by increase in the cone angle.

It means that the radial effects of compaction decreases with increase in the cone angle. Flat tampers obviously owe more radial influence compared to the conical ones. It implies that although more improvement depths can be reached through using conical tampers, the distance between adjacent tamping points must be reduced to induce an overlap between stress bubbles under the tampers and obtaining uniform soil improvement. Base on the analyses results, maximum radial distance of improvement occurs at the ground surface and is about 3.5 d where d is the tamper diameter. More crater volume of flat tamper compared to conical ones also implies that more soil is needed for filling the craters in ironing stage before starting the next phase of compaction.

Figure 9 shows plastic strain contours under flat and conical tampers ($\alpha = \varphi$) in different soils. The results demonstrate increase in improvement depth by using conical tampers compared to the flat ones. The figure also confirms the greatest improvement depth for very loose sand and the smallest in medium dense soil.

The other important parameter which must be studied is vibrations induced during dynamic compaction operations. Noise and vibrations can be hazardous to the adjacent structures or lifelines, buried facilities or pipelines and also suffer the nearby residents. In order to investigate vibrations induced during dynamic compaction process, peak particle velocity (PPV) was used as the main controlling parameters. It has been widely considered in previous studies to evaluate the amount of vibrations during compacting process (Hwang and Tu, 2006).

Figure 10 indicates variation of PPV in 5th blow count with radial distance from tamping centerline for different soil types. As it can be seen, although PPV decreases by increase in radial distance, increase in cone angle increases PPV in all radial distances. For very loose sand, PPV of conical tamper is averagely 18.6% more than flat one. The rate is 23.3% and 23.5% for loose and medium dense sands, respectively. Moreover, PPV was obtained more in denser sand compared to the looser soil.

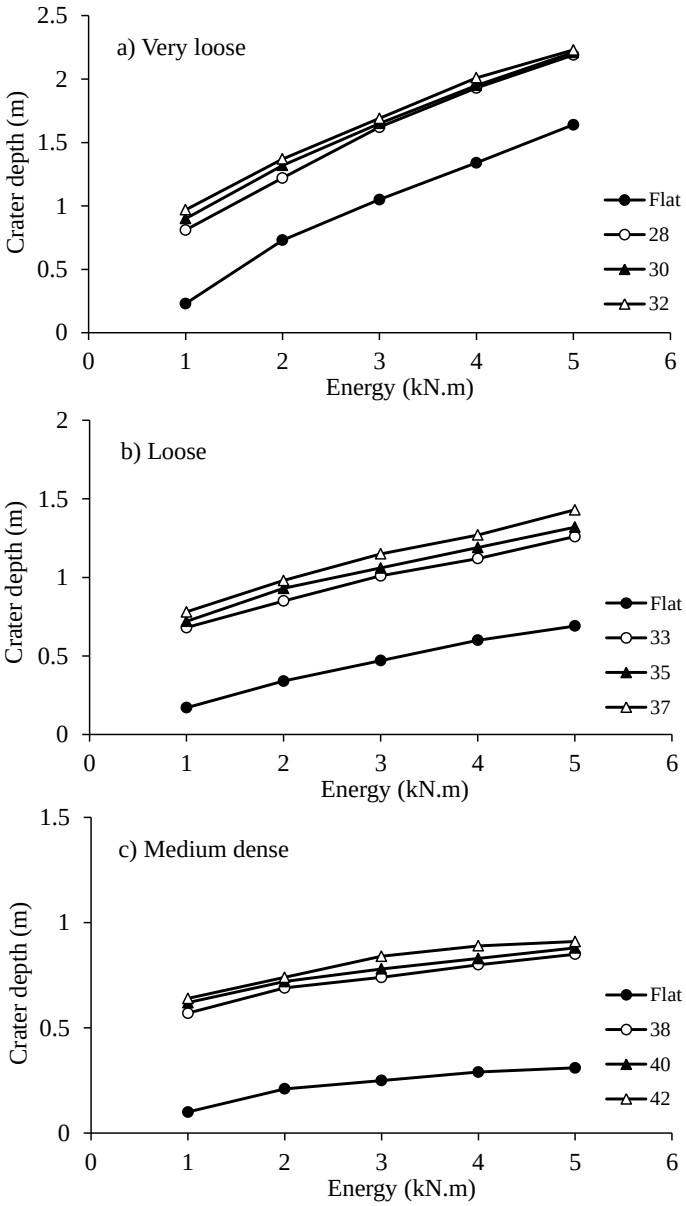

Fig. 7. Comparison of crater depths induced by tampers in different soil types

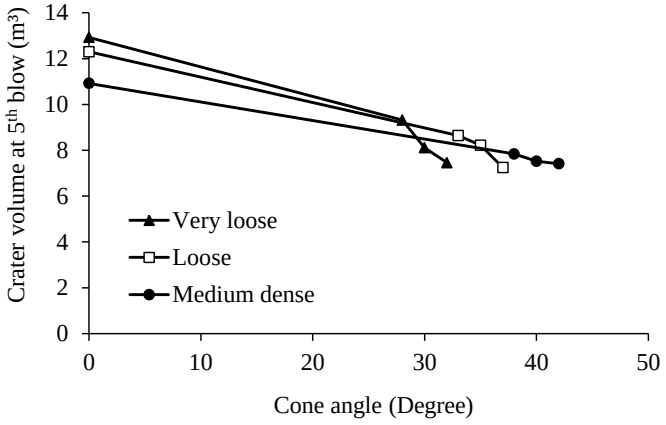

Fig. 8. Variation of crater volume with cone angle in different soil types

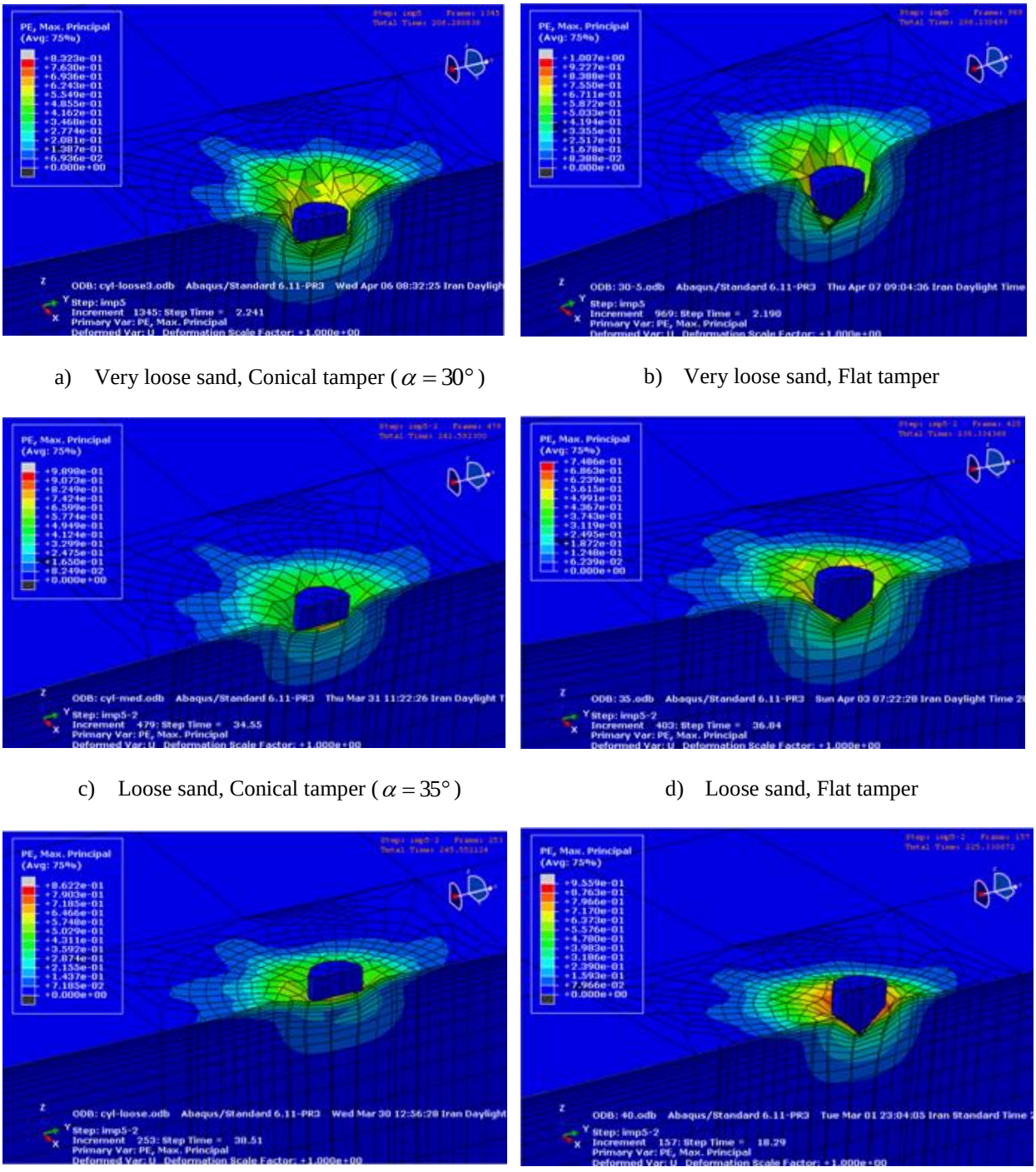

a) Very loose sand, Conical tamper ($\alpha = 30°$)

b) Very loose sand, Flat tamper

c) Loose sand, Conical tamper ($\alpha = 35°$)

d) Loose sand, Flat tamper

e) Medium sand, Conical tamper ($\alpha = 40°$)

f) Medium sand, Flat tamper

Fig. 9. Maximum principal strain contours at 5th blow count created in very loose, loose and medium sand by a 30 ton tamper falling from the 20 m height

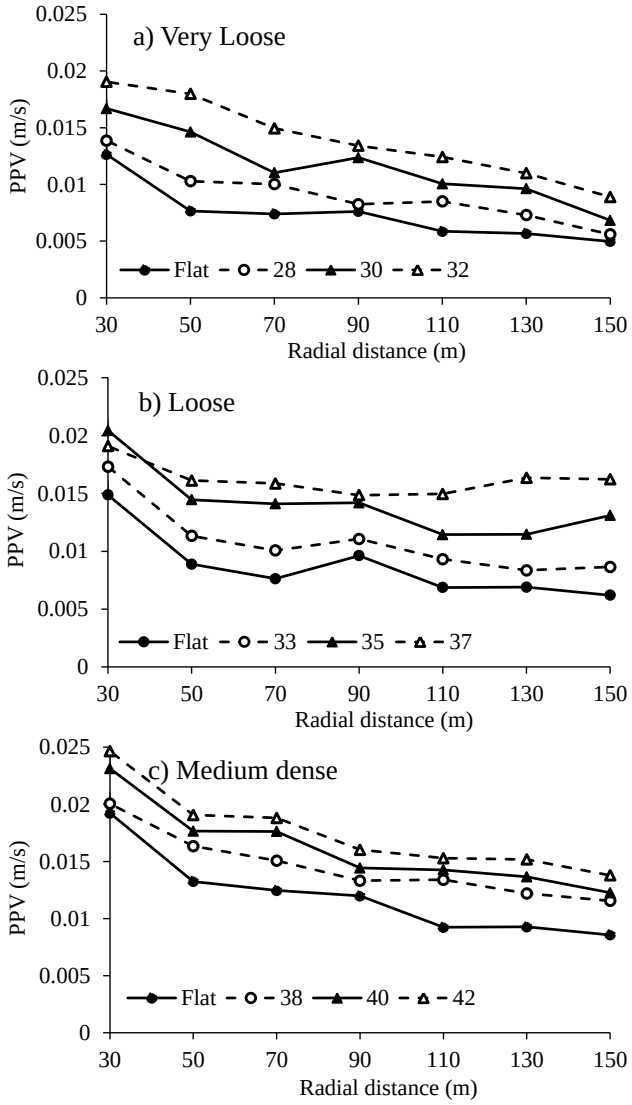

Fig. 10. Variation of PPV in 5th blow count with radial distance from tamper centerline for various cone angles and different soil types

CONCLUSIONS

- Use of conical tampers result in more crater depths compared to the flat ones. It is due to the lower contact area and concentration of stresses at the cone tip.
- Contrary to vertical depth of improvement, in radial direction, flat tampers are more effective compared to the inclined ones. In this regard, lower tamping distances must be applied for conical tampers to reach overlap in radial directions, however, number of impacts decreases for conical tampers due to the greater depths of improvement.
- Due to the large time step between two successive blows in dynamic compaction, PPV at different points in each blow was independent of the previous blows. The highest particle velocity was recorded at the nearest point and decreased with increase in radial distance.
- Induced PPV during compaction using conical tampers was more compared to the flat ones in all radial distances. Also maximum PPV was observed for dense sand compared to the looser soil.

REFERENCES

Ardeshir Behrestaghi, A., Eskandari Ghadi, M. and Vaseghi-Amiri, J. (2013). "Analytical solution for a two-layer transversely isotropic half-space affected by an arbitrary shape dynamic surface load", *Civil Engineering Infrastructures Journal*, 46(1), 1-14.

Arslan, H., Baykal, G. and Ertas, O. (2007). "Influence of tamper weight shape on dynamic compaction", *Ground Improvement*, 11(2), 61-66.

Bement, R.A.P. and Selby, A.R. (1997). "Compaction of granular soils by uniform vibration equivalent to vibro driving of piles", *Geotechnical and Geological Engineering Journal*, 15(2), 121-43.

Feng, T.W., Cheng, K.H., Su, Y.T. and Shi, Y.C. (2000). "Laboratory investigation of efficiency of conical-based pounders for dynamic compaction", *Geotechnique*, 50(6), 667-674.

Ghanbari, E. and Hamidi, A. (2014). "Numerical modelling of rapid impact compaction in loose sands", *Geomechanics and Engineering*, 6(5), 487-502.

Ghassemi, A., Pak, A. and Shahir, H. (2009). "A numerical tool for design of dynamic compaction treatment in dry and moist sand", *Iranian Journal of Science and Technology*, 33(B4), 313-326.

Hwang, J.H. and Tu, T.Y. (2006). "Ground vibration due to dynamic compaction", *Soil Dynamics and Earthquake Engineering*, 26(5), 337-346.

Li, W., Gu, Q., Su, L. and Yang, B. (2011). "Finite element analysis of dynamic compaction in soft foundation", *Procedia Engineering*, 12, 224-228.

Lukas, R.G. (1986). "Dynamic compaction for highway construction", Report No. FHWA/RD-86/133. Washington D.C., Federal Highway Administration, Department of Transportation, USA.

Luongo, V. (1992). "Dynamic compaction: Predicting depth of improvement", *Geotechnical Special Publication*, 2(30), 927-939.

Mayne, P.W., Jones, J.S. and Dumas, J.C. (1984). "Ground response to dynamic compaction", *Journal of Geotechnical Engineering, ASCE*, 110(GT6), 757-773.

Menard, L. and Broise Y. (1975). "Theoretical and practical aspects of dynamic consolidation", *Geotechnique*, 25(1), 3-18.

Merrifield, C.M. and Davis, M.C.R. (2000). "A study of low-energy dynamic compaction: Field trials and centrifuge modeling", *Geotechnique*, 50(6), 675-681.

Pan, J.L. and Selby, A.R. (2002). "Simulation of dynamic compaction of loose granular soil", *Advances in Engineering Software*, 33(7-10), 631-640.

Pourjenabi, M., Ghanbari Alamouti, E. and Hamidi, A. (2013). "Numerical modeling of dynamic compaction in dry sand using different constitutive models", *4th International Conference on Computational Methods in Structural dynamics and Earthquake Engineering*, Greece.

Pourjenabi, M. and Hamidi, A. (2015). "Numerical modeling of dynamic compaction process in dry sands considering critical distance from adjacent structures", *Structural Engineering and Mechanics*, 56(1), 49-56.

Qiao, J. and Li, L. (2011). "Model test study on vibration transferring of dynamic compaction of hydraulic filling foundation reinforcement", *Systems Engineering Procedia*, 1, 61-68.

Raoofian Naeeni, M. and Eskandari Ghadi, M. (2016). "A potential method for body and surface wave propagation in transversely isotropic half and full spaces", *Civil Engineering Infrastructures Journal*, 49(2), 263-288.

Rezaei, M., Hamidi, A. and Farshi Homayoun Rooz, A. (2016). "Investigation of peak particle velocity variations during impact pile driving process", *Civil Engineering Infrastructures Journal*, 49(1), 59-69.

Shafiei, M. and Khaji, N. (2015). "An adaptive physics-based method for the solution of one-dimensional wave motion problems", *Civil Engineering Infrastructures Journal*, 48(2), 217-234.

Smoltczyk, U. (1983). "Deep compaction", *8th European Conference on Soil Mechanics and Foundation Engineering*, Finland.

van Impe, W.F. (1989). *Soil improvement techniques and their evolution*, A.A. Balkema, Rotterdam.